Asian Journal of Pharmaceutical Sciences 17 (2022) 855–866

Available online at www.sciencedirect.com

ScienceDirect

journal homepage: www.elsevier.com/locate/AJPS

Original Research Paper

Protein corona mediated liposomal drug delivery for bacterial infection management

Qianwen Shao[a], *Tianhao Ding*[a], *Feng Pan*[a], *Guanghui Li*[c], *Shun Shen*[b,*], *Jun Qian*[a,*], *Changyou Zhan*[a,b], *Xiaoli Wei*[a,*]

[a] *School of Pharmacy & Department of Pharmacology, School of Basic Medical Sciences, Fudan University, Shanghai 201203, China*
[b] *Department of Pharmacy & Center for Medical Research and Innovation, Shanghai Pudong Hospital, Fudan University Pudong Medical Center, Shanghai 201399, China*
[c] *Department of Pharmacy, Jing'an District Central Hospital of Shanghai, Shanghai 200040, China*

ARTICLE INFO

Article history:
Received 18 July 2022
Revised 10 October 2022
Accepted 15 October 2022
Available online 5 November 2022

Keywords:
Liposome
Protein corona
Complement
Methicillin-resistant staphylococcus *aureus*
Liposome-bacteria interaction

ABSTRACT

Liposomes have been widely investigated as a class of promising antibiotic delivery systems for the treatment of life-threatening bacterial infections. However, the inevitable formation of protein corona on the liposomal surface can heavily impact *in vivo* performance. A better understanding of the effects of protein corona on liposomal behavior can significantly improve antibacterial liposomal drug development. Here, the critical role of protein corona in mediating liposome-bacteria interactions was elucidated. Adsorption of negatively charged protein on cationic liposome weakened electrostatic attraction-enhanced liposomal binding to the bacteria. Cumulative complement deposition on anionic liposome composed of phosphatidylglycerol (DSPG sLip) contributed to a superior binding affinity of DSPG sLip to planktonic bacteria and biofilms, which was exploited to enhance bacteria-targeted drug delivery. In both *S. aureus*-related osteomyelitis and pneumonia mice models, DSPG sLip was demonstrated as a promising antibiotic nanocarrier for managing MRSA infection, indicating the benefits of lipid composition-based protein corona modulation in liposomal antibiotic delivery for bacterial infection treatment.

1. Introduction

Pathogenic bacterial infection poses a severe threat to public health and human life. The multidrug-resistant bacterial infection and difficult-to-treat infection further brought big challenges to clinical practice [1,2]. The antibiotics abuse led to a continuous emergence of drug-resistant bacteria strains, increasing the difficulties in treating bacterial infections. According to the recent study in The Lancet, there were about 1.2 million deaths from antibiotic-resistant bacterial infections in 2019 [3]. It takes much time and effort for

* Corresponding authors.
E-mail addresses: nanocarries@gmail.com (S. Shen), qianjun@fudan.edu.cn (J. Qian), xlwei@fudan.edu.cn (X.L. Wei).
Peer review under responsibility of Shenyang Pharmaceutical University.

https://doi.org/10.1016/j.ajps.2022.10.003

the development of novel small-molecule antibiotics. Due to reduced profit motivations and strict regulatory requirements for drug companies to develop new antibiotics, the number of new antibiotics that the FDA approved annually has slowed to a trickle while the rate of bacterial mutation is growing exponentially [4–6]. As warned by CDC, the world may enter a "post-antibiotic" era if no action is seriously taken [7]. In this case, the clinicians start to reconsider old antibiotics which are not used as first-line treatments due to their poor pharmacokinetics or toxicity issues. However, the clinical application of conventional antibiotics is usually limited by their poor solubility, bioavailability, tissue penetration, stability, and toxicities. Sufficient delivery of antibiotics to the infected sites could minimize the risks of systemic toxicity and reduce the likelihood of developing resistance. Hence, an appealing strategy is the combination of available antibiotics with nanotechnology, which is widely adopted to help improve the therapeutic index.

Besides drug resistance, the existence of biological barriers such as cell membranes, mucus, and bacterial biofilms prevents the successful accumulation of therapeutics to the sites of infection, limiting bacterial killing efficiency and making some infections difficult to treat [8,9]. Especially, bacterial cells can adhere to the surface of material or tissue and be packed in extracellular polymeric substances, thus forming bacterial biofilms [10,11]. By acting as a physical and enzymic barrier, biofilms protect bacteria from access of free antimicrobial agents and the host immune system, posing big challenges for clinical treatment. It is known that biofilm-mediated infections are hard to eradicate by conventional antibiotic treatment and it usually requires long-term and high dosage of antibiotic therapy. As reported, the minimum bactericidal concentration for bacteria in the biofilm was much higher than that for planktonic bacteria [12]. The prolonged and aggressive antibiotic treatment further increases the likelihood of drug resistance and toxicity. Collectively, these facts underscore the undisputed demand for better delivery strategies to deliver antibacterial agents to the biofilm-associated bacteria for advanced efficacy and reduced side effects.

Hence, combating bacterial infections requires not only an appropriate antibiotic but also an appropriate delivery system. The liposome has been long-term investigated as a promising drug delivery vehicle to improve the safety and effectiveness of various drugs including antibiotics [13,14]. Liposomes are nano-sized spherical vesicles made up of phospholipids and cholesterol. Hydrophilic drugs could be loaded into the inner core and their hydrophobic lipid bilayer is responsible for entrapping insoluble agents. They were widely used as biodegradable drug carriers for targeted delivery, and also the most commonly-used antibiotics delivery vehicles [15,16]. Among these, various liposomal vancomycin formulations were fabricated for methicillin-resistant *staphylococcus aureus* (mrsa) infection management to improve therapeutic activity and reduce its notable nephrotoxicity and ototoxicity [17,18]. Based on their physicochemical properties including surface charge and modification, direct and indirect interactions between liposomes and bacteria have been investigated [19]. Positively charged liposomes were reported to be capable of targeting negatively charged bacteria by electrostatic interaction [20,21].

it is widely accepted that the surface of nanomedicines would be inevitably opsonized and masked by layers of plasma proteins to form the "protein corona" once entering into the blood stream [22,23]. Especially for non-peglyated liposomes, heavy opsonization by plasma protein and subsequent reticuloendothelial system (RES) uptake lead to rapid blood clearance, presenting a major barrier to drug delivery. Although peg grafted surface has been proven to help limit protein opsonization, various studies have found that peglyation cannot fully prevent protein adsorption [24]. The composition and amount of protein corona would vary a lot with nanomedicines in terms of material, shape, size, and surface modification, et cetera [25]. The *in vivo* fate of nanomedicine such as blood circulation, organ biodistribution, cellular interaction and intracellular transport is substantially affected by the adsorbed proteins. Researchers have been attempting to identify key plasma proteins and their crucial role in the regulation of liposomal *in vivo* performance. Recent studies clarified that opsonization by immunoglobulins accelerates the rapid recognition and clearance of liposomes by RES, and even causes further immune responses [26,27]. On the contrary, the adsorption of albumin and apolipoprotein could prolong their blood circulation and improve biocompatibility [28]. Understanding how liposomes interact with the biological milieu and how protein corona affects the interaction between liposomes and bacteria are crucial for the rational development of liposomal antibiotics for managing bacterial infection. Here, the effect of protein corona on the interactions between liposomes and bacteria was explored. Specific enriched protein mediated liposome-MRSA interaction was actively exploited here to enhance bacteria-targeted antibiotic delivery.

2. Materials and methods

2.1. *Materials*

DSPG (1, 2-distearoyl-sn–glycero-3-phosphoglycerol), DPPG (1,2-dipalmitoyl-sn–glycero-3-phosphoglycerol), DMPG (1, 2-dimyristoyl-sn–glycero-3-phosphoglycerol), DSPC (1,2-distearoyl-sn–glycero-3-phosphocholine), DPPC (1, 2-dipalmitoyl-sn–glycero-3-phosphocholine), HSPC (hydrogenated soybean phosphatidylcholine), mPEG2000-DSPE, DOTAP (1, 2-dioleoyl-3-trimethylammonium-propane) and cholesterol were purchased from A.V.T. Pharmaceutical, Co., Ltd. (Shanghai, China). DiD (DiIC18(5), 1,1′-dioctadecyl-3,3,3′,3′-tetramethylindodicarbocyanine perchlorate), HRP-labeled Goat Anti-Rabbit IgG, TMB (3,3′,5,5′-Tetramethylbenzidine), DAPI, Fast Silver Stain Kit and SDS-PAGE sample loading buffer were acquired from Beyotime Biotechnology (Nantong, China). DiI (DiIC18(3), 1,1′-dioctadecyl-3,3,3′,3′-tetramethylindocarbocyanine perchlorate), Sephadex G50 and BCA Protein Assay Kit (Cat# 71,285) were from Sigma (St. Louis, MO). Vancomycin was obtained from Dalian Meilun Biotechnology Co., Ltd. (Dalian, China). 4%–20% gradient precast polyacrylamide gels and precision plus protein dual color standards were

from BIO-RAD (Hercules, CA). Rabbit anti-mouse C3 antibody (ab200999) was purchased from Abcam (Cambridge, MA). Alexa Fluor® 488 anti-mouse Ly-6 G Antibody and Alexa Fluor® 647 anti-mouse F4/80 Antibody were from Biolegend (San Diego, CA). Sheep red blood cell (SRBC, 4%) was acquired from Beijing Solarbio Science & Technology Co., Ltd. (Beijing, China).

2.2. Animals

Male ICR mice (20–22 g) were purchased from Shanghai SLAC laboratory animal Co. LTD. All animal experiments were carried out in accordance with the Guidelines of the Care and Use of Laboratory Animals of Fudan University with approval from the Animal Ethics Committee of Fudan University.

2.3. Preparation of liposomes

PC/cholesterol/mPEG2000-DSPE (52:43:5) and DOTAP/HSPC/cholesterol/mPEG2000-DSPE (20:32:43:5) was dissolved in chloroform. PG/cholesterol/mPEG2000-DSPE (52/43/5) was dissolved in a mixed solvent of chloroform and water (200:1) at 60 °C, followed by rotary evaporation to form thin films. And then the lipid films were hydrated with PBS at 60 °C and subsequently extruded through Whatman polycarbonate membranes. DiD/DiI-labeled liposomes were fabricated by a similar method, except that DiD/DiI was added before rotary evaporation. Van-loaded liposomes were prepared via a freeze-thaw method. For PC sLip and TAP sLip, 10 mg/ml vancomycin was added into the dried lipid film. For PG sLip, the hydrated lipid dispersion was mixed with 20 mg/ml vancomycin in PBS and experienced a freezing and thaw process. Free vancomycin was removed by Sephadex G50 column after 8–9 freeze-thaw cycles. The vancomycin concentration and loading capacity were measured by the HPLC as previously reported [18] (Agilent Technologies HPLC-1260). The liposomal size and zeta potential were measured by Malven Zetasizer Nano ZS90 and the liposomal size in 50% mice serum (1 mg/ml lipid concentration) was measured by NanoSight NS300 (Malven). *In vitro* vancomycin release studies were carried out by a dialysis method [18].

2.4. Binding of liposomes to bacteria

Fluorescent dye labeled PG sLip, PC sLip and TAP sLip was preincubated with PBS, serum or bronchoalveolar lavage fluid (BALF) at 37 °C for 1 h. 50 µl mixture was incubated with 3×10^7 CFU MRSA in 500 µl TSB at 37 °C for another 1 h. Bacteria with bound liposomes were obtained by centrifugation at 5000 g. After three times wash with PBS, the pellet was resuspended in PBS. The bacteria were stained with DAPI, followed by flow cytometry (Agilent NovoCyte). The fluorescent signal of MRSA bound with liposomes was visualized by confocal microscopy (LSM710, Zeiss).

2.5. Binding of liposomes to MRSA biofilms

In brief, 1×10^6 CFU MRSA in 100 µl TSB were cultured in 96-well plate for 24 h to establish bacteria biofilms. Free bacteria were removed by PBS washing. The biofilms were then incubated with DiI labeled liposomes preincubated with PBS or ICR mouse serum at 37 °C for 1 h, followed by thrice wash. The biofilm was then stained by DAPI and subjected to fluorescence microscope observation (DMI4000D, Leica) and 3D rendering (LSM710, Zeiss).

2.6. Characterization of protein corona

Liposomes (14 mg/ml lipid concentration, 100 µl) were mixed with 100 µl health ICR mouse serum and then incubated at 37 °C for 1 h. Subsequently, chilled 1 × PBS was added into the mixture and liposome-protein complex was isolated via centrifugation at 14 000 g. The liposome-protein complex was washed three times and then resuspended in 30 µl PBS. Electrophoresis was then carried out and followed by fast silver staining. Western Blotting was performed and probed using anti complement C3 antibody.

2.7. Hemolytic complement activity assay

Serial dilutions of PG sLip, PC sLip or TAP sLip were incubated with rat serum at 37 °C for 1 h, followed by 30 min incubation with 4% sensitized SRBC. Then the mixture was centrifugated for 5 min at 3000 g and the absorbance of the supernatant was measured at 542 nm.

2.8. In vivo efficacy study

To establish MRSA osteomyelitis mice model, ICR mice were challenged with 2 µl of 1×10^6 CFU MRSA in the medullary cavity of the femur. After 5 d, the mice ($n = 7$–8) were intravenously injected with vancomycin loaded PG sLip, PC sLip, TAP sLip, free vancomycin (vancomycin dose 10 mg/kg) and PBS respectively, every four hours, for three doses. Femur specimens were collected at 4 h post treatment and flushed with 500 µl PBS to obtain the medullary cavity lavage fluid. Serial dilutions of the medullary cavity lavage fluid were plated on TSB agar plates for bacterial enumeration.

For MRSA pneumonia murine model establishment, ICR mice ($n = 6$) were intratracheally inoculated with 50 µl of 2×10^6 CFU MRSA and then intratracheally administered with 50 µl PG sLip/Van, PC sLip/Van, TAP sLip/Van, free vancomycin (vancomycin dose 0.75 mg/kg) or PBS. The survival was monitored and recorded over a period of 48 h. Lungs of survived mice were then collected and homogenized with PBS at 4 °C for bacterial enumeration.

2.9. Pharmacokinetics and biodistribution study

To study the liposomal pharmacokinetics *in vivo*, ICR mice ($n = 4$) were injected with DiD labeled PG sLip, PC sLip and TAP sLip (1 mg DiD/kg) respectively. Plasma was collected by using EDTA as anticoagulant at different time points for fluorescent intensity measurement (Ex = 640 nm, Em = 680 nm). The mice were then perfused with PBS at 24 h post injection. The main organs were homogenized, and the fluorescent intensity was measured using a fluorescence spectrophotometer (Tecan).

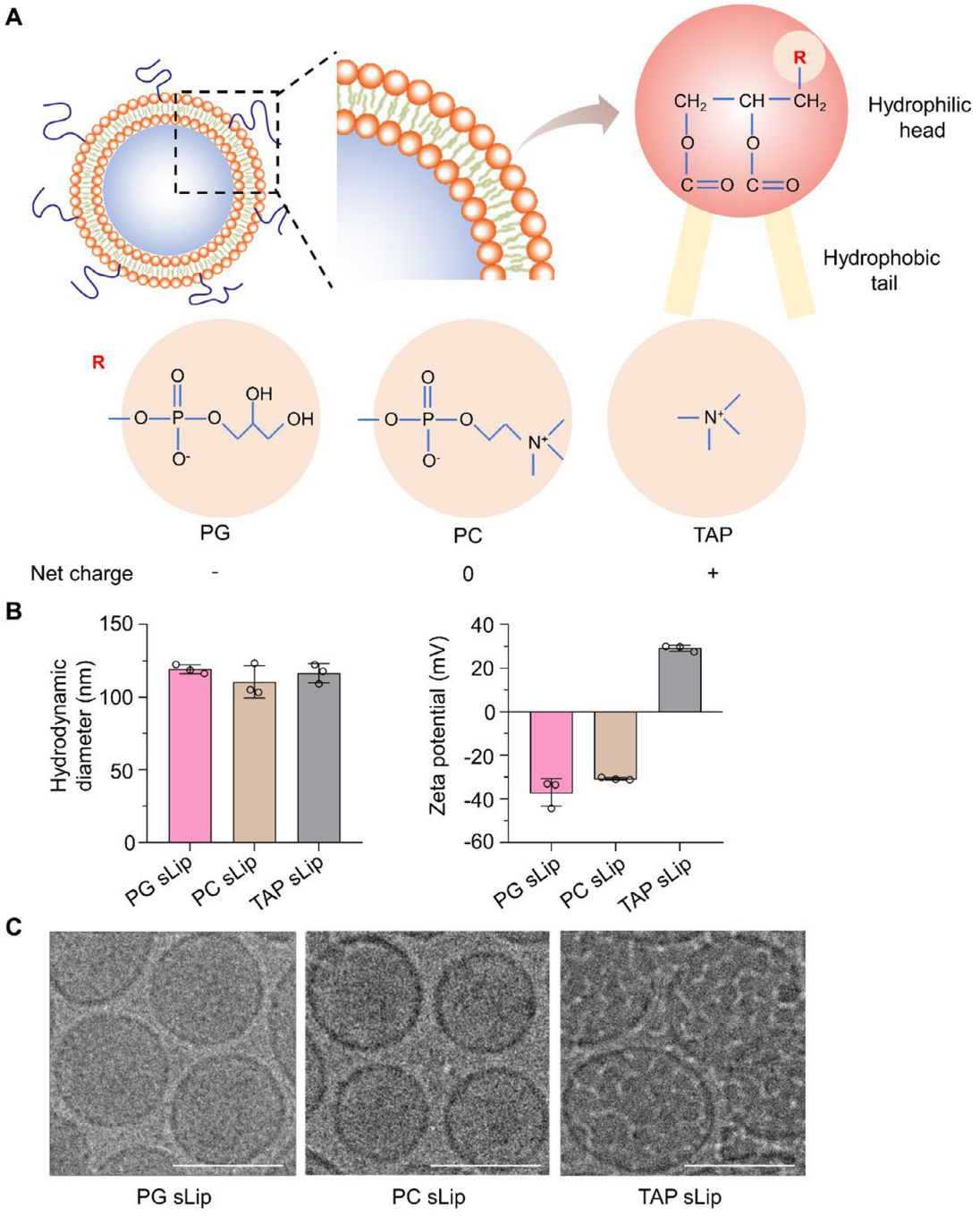

Fig. 1 – Characterization of PG sLip, PC sLip, and TAP sLip. (A) Schematic illustration of liposomes composed of DSPG, DSPC and DOTAP lipids and their net charges. (B) Size and zeta potential of liposomes. (C) Representative cryo-EM images of three populations of liposomes. (scale bar = 100 nm).

2.10. *Safety evaluation*

To evaluate the safety of liposomal vancomycin formulations, mice ($n = 4$) were injected with three population of vancomycin loaded liposomes (10 mg/kg). Blood routine test was performed after 24 h and biochemical analysis of mice serum was carried out to assess the hepatic and renal function. To further evaluate pulmonary toxicity following lung exposure to vancomycin loaded liposomes, mice were intratracheally administered with 50 μl PG sLip/Van, PC sLip/Van, TAP sLip/Van or free vancomycin (0.75 mg/kg). BALF was then collected and then spun at 3000 g to harvest the cells. The cell pellets were resuspended by PBS and stained with either Alexa Fluor® 488 labeled anti-Ly-6 G antibody or Alexa Fluor® 647 labeled anti-F4/80 antibody for neutrophils and macrophages counting.

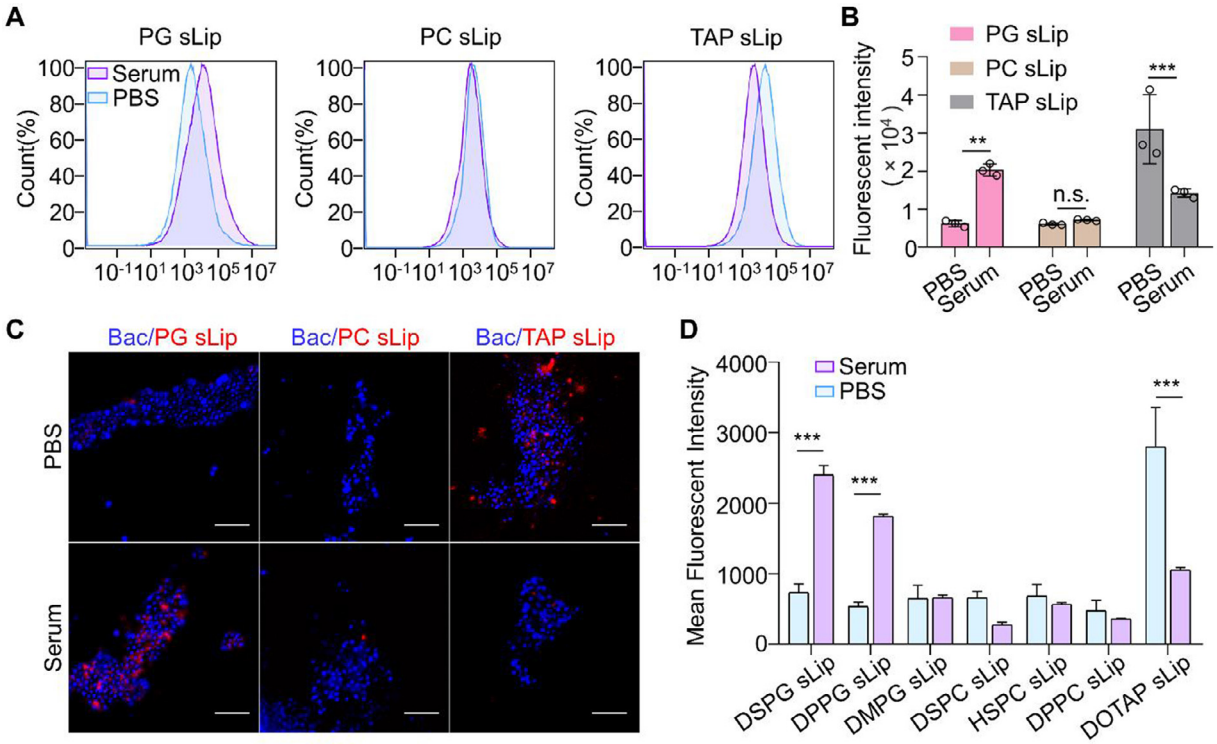

Fig. 2 – Liposome binding to MRSA. (A) Representative flow cytometry histograms and (B) Fluorescent quantification of MRSA bound with PG sLip, PC sLip, and TAP sLip either preincubated with PBS or mouse serum. (C) Representative fluorescent images of liposomes bound to MRSA. (scale bar = 10 μm). (D) Mean fluorescent intensity (MFI) of MRSA bound with different liposomes either preincubated with PBS or mouse serum analyzed by flow cytometry ($n = 3$).

2.11. *Statistical analysis*

Data was presented as mean ± SD and analyzed by ANOVA with GraphPad Prism 8.0.1. In all analysis, levels of significance were set at $P < 0.05$ (n.s.: non-significance, $^{*}P < 0.05$, $^{**}P < 0.01$ and $^{***}P < 0.001$).

3. Results and discussion

3.1. *Preparation and characterization of liposomes*

To form the liposomal bilayer, phospholipids line up next to each other with their hydrophilic heads on the outside of the vesicles, thus various head groups on the liposome surface have significant influences on protein corona formation and interaction with bacteria. Here, liposomes with varying surface properties were prepared by changing the head groups of phospholipids. As model systems, anionic lipid phosphatidylglycerol DSPG, neutral lipid phosphatidylcholine DSPC, and cationic lipid DOTAP were employed here to endow liposomes with various surface properties (Fig. 1A). Different populations of liposomes were fabricated by thin-film hydration and extrusion method, denoted as PG sLip, PC sLip, and TAP sLip. All three populations of liposomes had a hydrodynamic diameter at about 120 nm with narrow particle distributions. Due to the addition of anionic lipid mPEG-DSPE for long blood circulation, all the formulations, except TAP sLip, presented negatively charged surface in deionized water according to the zeta potential measurement data (Fig. 1B). The representative cryo-EM images revealed that all three populations of liposomes were spherical vesicles formed by phospholipid layered membrane (Fig. 1C).

3.2. *Protein corona on PG sLip targets MRSA planktonic bacteria*

To investigate the influence of formed protein corona on the interplay between liposome and bacteria, fluorescent dye DiD labeled liposomal formulations were pretreated with ICR mouse serum and subsequently incubated with MRSA planktonic bacteria. After incubation, the bacteria were thoroughly rinsed and subjected to flow cytometry analysis and fluorescent intensity measurement (Fig. 2A and 2B). The data revealed that TAP sLip exhibited much higher binding affinity to MRSA in PBS compared to the other two groups, which may be attributed to electrostatic interactions between the cationic TAP sLip and negatively charged *S. aureus*. However, upon pre-incubation with mouse serum, the amount of TAP sLip bound on the bacteria was significantly decreased. It is widely accepted that favorable electrostatic interaction is one of the main forces for protein adsorption on liposomes. Negatively charged proteins tend to be adsorbed on cationic membranes and the amount of protein deposited might increase with the increasing surface charge density [29]. Here, zeta potential of TAP sLip shifted toward negative

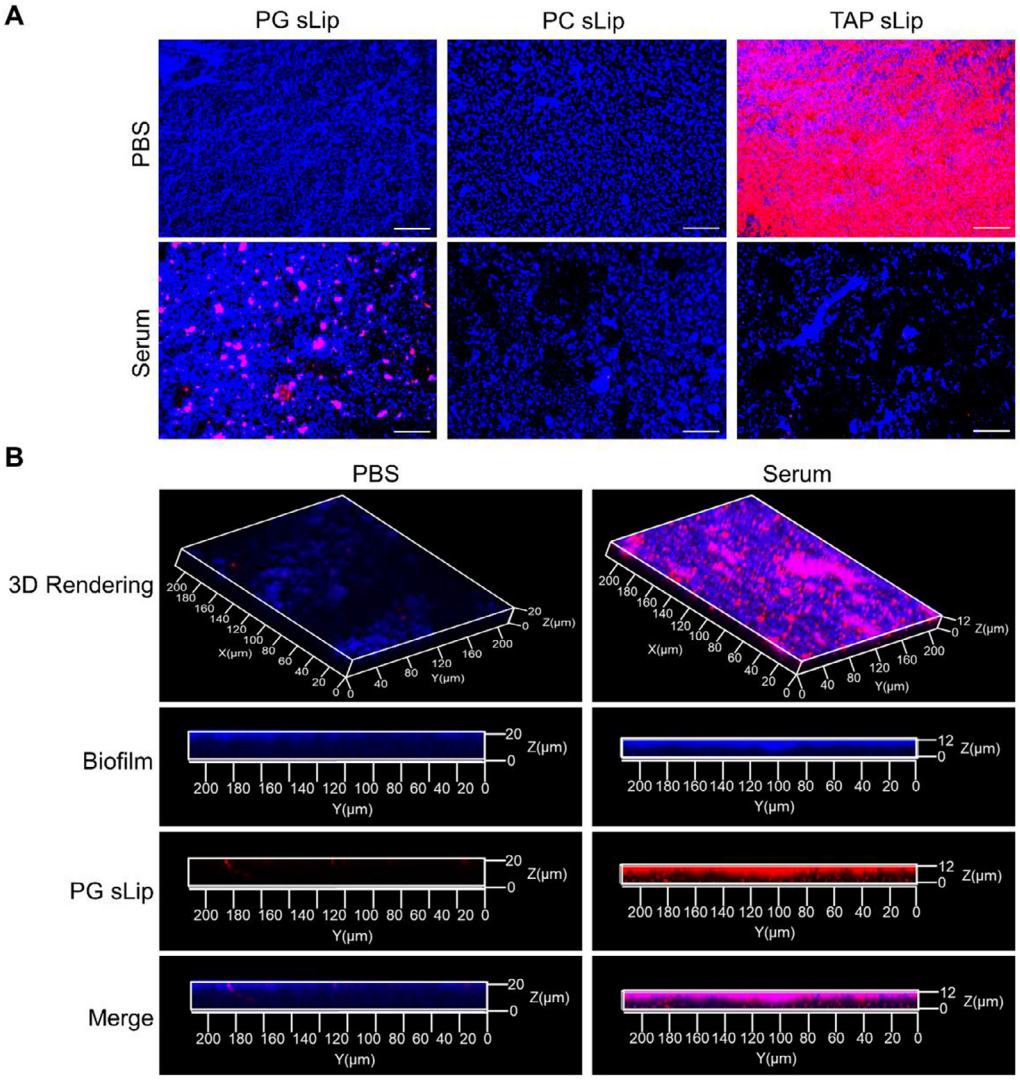

Fig. 3 – Liposome binding to MRSA biofilm. (A) Fluorescent imaging of liposomes bound to MRSA biofilm (Blue = MRSA bacteria, Red = liposomes, scale bar = 100 μm). (B) 3D rendering microscopic observation of MRSA biofilm (blue) and DiI-labeled liposomes (red) by laser scanning confocal microscope.

values due to surface adsorption of plasma proteins (Fig. S1), thus weakening the electrostatic attraction-mediated liposomal binding to the bacteria. Interestingly, PG sLip with formed protein corona demonstrated strong binding to MRSA planktonic bacteria as there was an obvious increase in the percentage of fluorescent positive MRSA in serum pretreated PG sLip group (53.4% ± 2.4%) *versus* that in PBS preincubated one (25.1% ± 4.3%).

Moreover, the binding of liposomes to MRSA in different conditions was further visualized using confocal microscopy (Fig. 2C). Sporadic red dots surrounding the bacteria in the PG sLip group preincubated with serum were clearly visible while little signal was observed in the PG sLip group preincubated with PBS, suggesting PG sLip retention and co-localization with the bacteria after protein corona formation. Overall, these results clearly indicated that adsorbed protein corona could mediate strong binding of PG sLip to MRSA.

To further investigate whether it was a peculiar situation for DSPG sLip, liposomes composed of anionic lipid phosphatidylglycerol with different lipid tail lengths including DSPG, DPPG, and DMPG were fabricated. Liposomes composed of neutral lipid phosphatidylcholine including DSPC, DPPC, and HSPC were used as controls. All populations of liposomes except DMPG liposome had a similar hydrodynamic diameter at around 120 nm (Fig. S2). DMPG liposome that has a shorter hydrocarbon chain (C14) displayed a smaller liposomal size of 94.8 ± 4.1 nm. All the formulations presented negatively charged surface by zeta potential measurement. According to the results of fluorescent intensity measurement, DSPG and DPPG liposomes were much more readily bound to MRSA after the formation of protein corona (Fig. 2D) while it was not the case for relatively small DMPG liposome. The interaction between phospholipid head groups on the relatively small DMPG liposome and serum complement protein C3 might be reduced as its amount that deposited

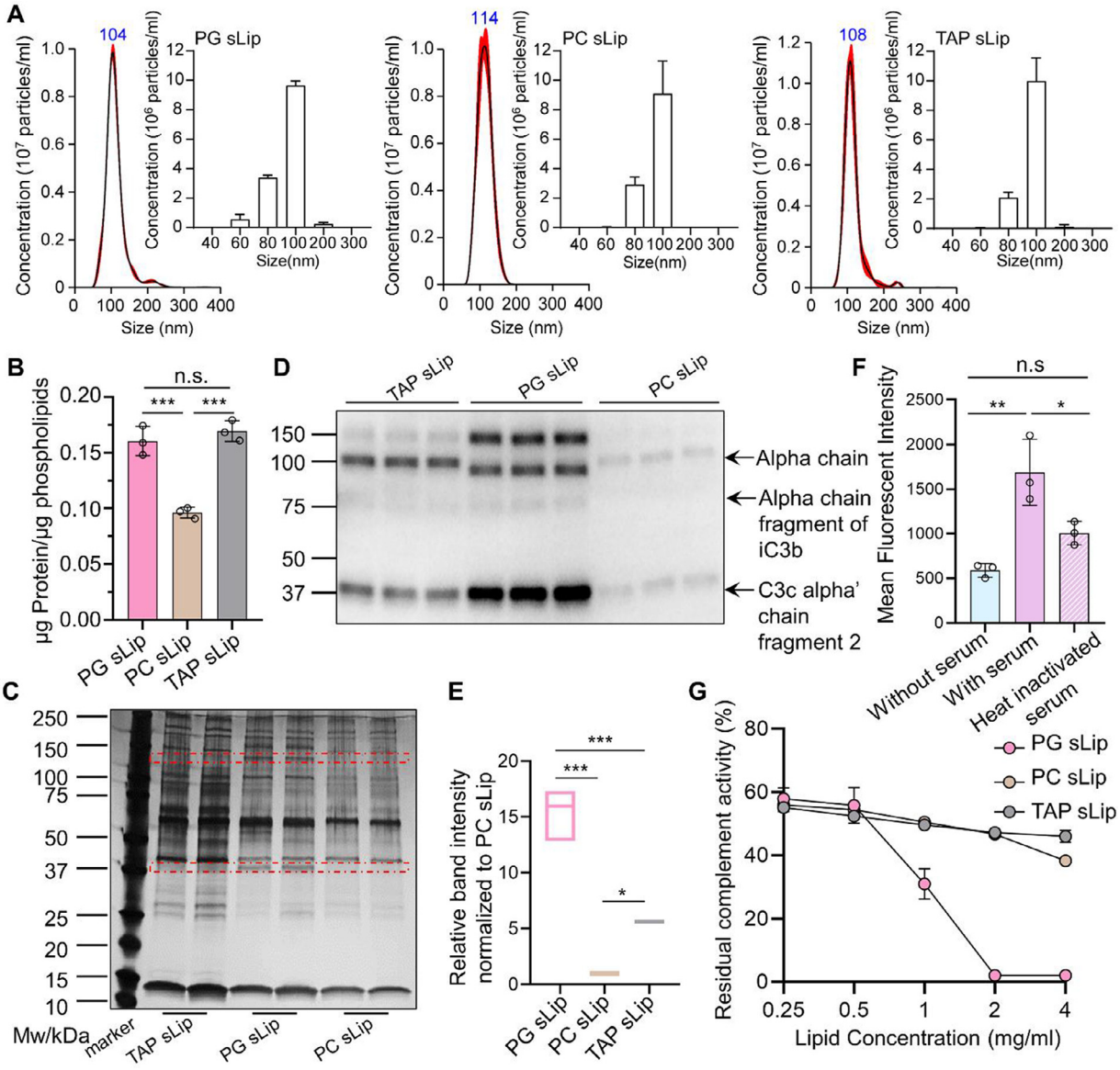

Fig. 4 – Adsorbed protein corona mediating interaction between liposomes and MRSA. (A) Size of DiI-labeled liposomes incubated with 50% serum measured by nanoparticle tracking analyzer. (B) The amount of serum protein adsorbed on the liposomes. (C) Protein corona SDS-PAGE. (D) Western blot of complement C3 on liposomal surface. (E) Quantification of adsorbed complement C3 by normalizing gray values. (F) Fluorescent quantification of MRSA bound with DiD-labeled PG sLip preincubated with PBS or mouse serum or heat inactivated serum. (G) Complement activation by various liposomes.

on DMPG liposome was significantly less than that on DSPG liposomes (Fig. S3). It is confirmed that DSPG sLip-protein complex possesses a particularly strong affinity with MRSA. However, upon preincubation with serum, the amounts of PC sLip bound on the MRSA either were slightly reduced or remained unchanged.

3.3. *PG sLip with formed protein corona exhibited strong binding to MRSA biofilm*

MRSA has been one of the most life-threatening pathogens due to its multidrug resistance and strong biofilm-forming capacity. In the biofilm, bacteria become much more resistant to antibiotic treatments and protected from body immune system [30]. In particular, the biofilm prevents access of antimicrobial agents to the bacteria by acting as a physical barrier, resulting in ineffective bacteria killing and biofilm eradication. To explore if the adsorbed protein on the PG sLip exerts a similar influence on the binding of liposome to the bacteria biofilm, an *in vitro* MRSA biofilm model was established and the binding experiments were performed by incubating MRSA biofilm with various populations of DiI-labeled liposomes with or without serum preincubation. The biofilm was then stained with DAPI for fluorescent

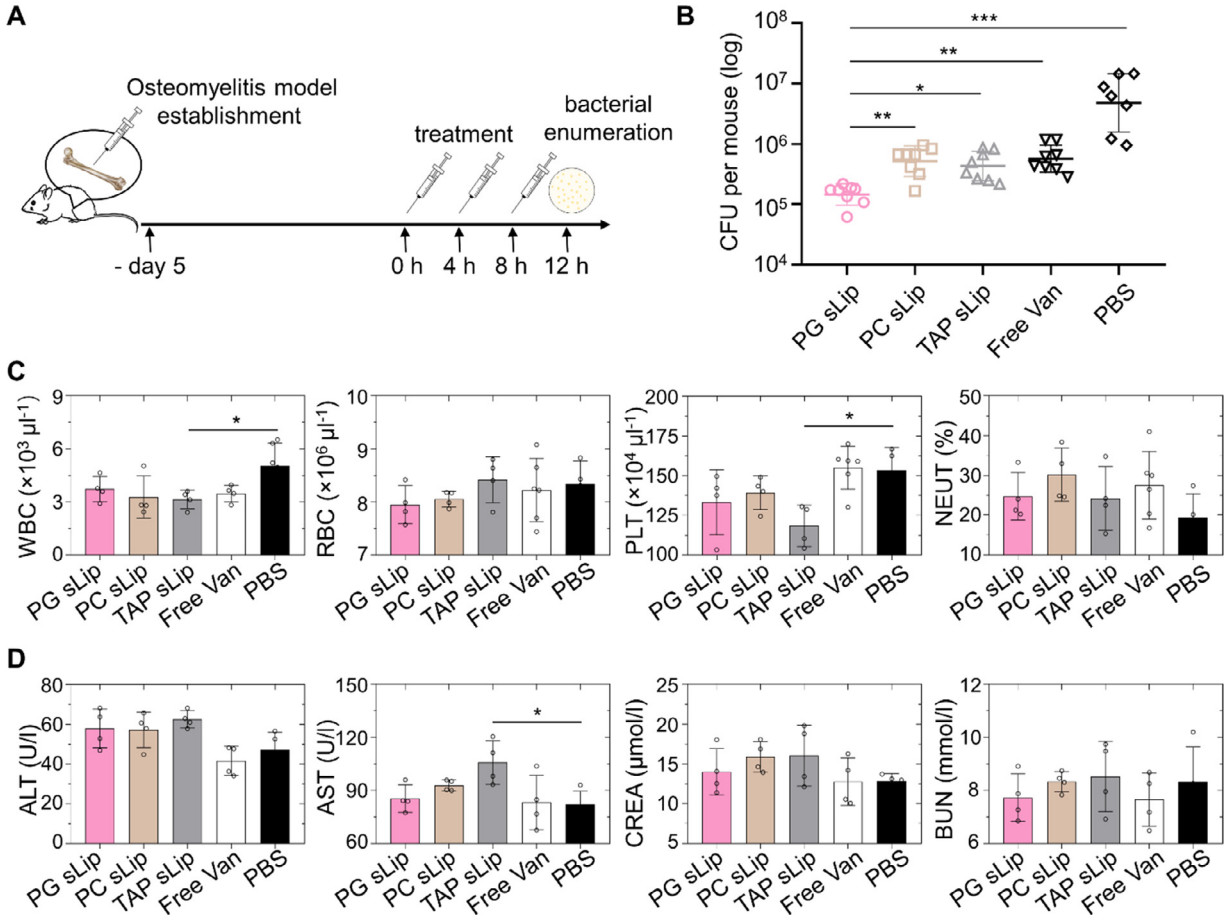

Fig. 5 – *In vivo* therapeutic efficacy and safety study. (A) Experimental design of the therapeutic efficacy study in the mouse model of MRSA osteomyelitis. (B) Bacterial load in the femur of mice bearing MRSA osteomyelitis after treatments. (C) Blood routine examination on white blood cells (WBC), red blood cells (RBC), platelets (PLT), and neutrophils of ICR mice. (D) Biochemical indexes of vital liver and kidney functions including ALT, AST, CREA and BUN.

microscopy imaging. As shown in Fig. 3A, there was barely red fluorescence observed neither on the surface nor inside the biofilms for PG sLip and PC sLip treated groups without serum preincubation, indicating that both populations of liposomes were incompetent for biofilm adhesion and penetration. In contrast, much more deposition of cationic TAP sLip was found than the other two populations of liposomes. It was consistent with previous reports that cationic particles were more likely to interact with and stick strongly to the negatively charged biofilm [31]. However, preincubation with serum shielded the positively charged surface of TAP sLip, resulting in weak binding to the biofilm. It is further confirmed here that the interaction between liposomes and bacterial biofilm is heavily modulated by the formed protein corona. In agreement with the planktonic bacteria binding study, the adherence of PG sLip to MRSA biofilm was significantly enhanced after serum preincubation. Furthermore, as shown in the z-stack images illustrating the overall distribution of PG sLip in the biofilm (Fig. 3B), serum-pretreated PG sLip was able to penetrate deeply and distribute in the biofilms. These data suggested that protein corona formed on PG sLip played important roles in determining the specific interactions with the MRSA biofilm.

3.4. *Complement in protein corona facilitates PG sLip strong binding with MRSA*

The protein corona largely determines the *in vivo* interaction between liposomes and the body. The composition of protein corona could be one of the key factors affecting biological identity of liposomes. Firstly, the influence of protein corona on the liposome size was studied by nanoparticle tracking analysis (NTA, NanoSight NS300). As shown in Fig. 4A, the protein corona formation did not exert a significant influence on the liposome size. All liposome-protein complexes exhibited very similar size. The amount of proteins deposited on three populations of liposomes was further quantified. It showed that proteins bound on PG sLip and TAP sLip were much more than that on PC sLip (Fig. 4B). Next, the adsorbed proteins were separated with SDS-PAGE, followed by subsequent silver staining (Fig. 4C). There was a significantly increased signal of protein bands at about 40 and 120 kDa in the serum pre-incubated PG sLip group, which were ascertained as complement fragments by western blotting (Fig. 4D). C3 complement and its degraded fragments were clearly visible in the protein corona formed on all three liposomes, which is

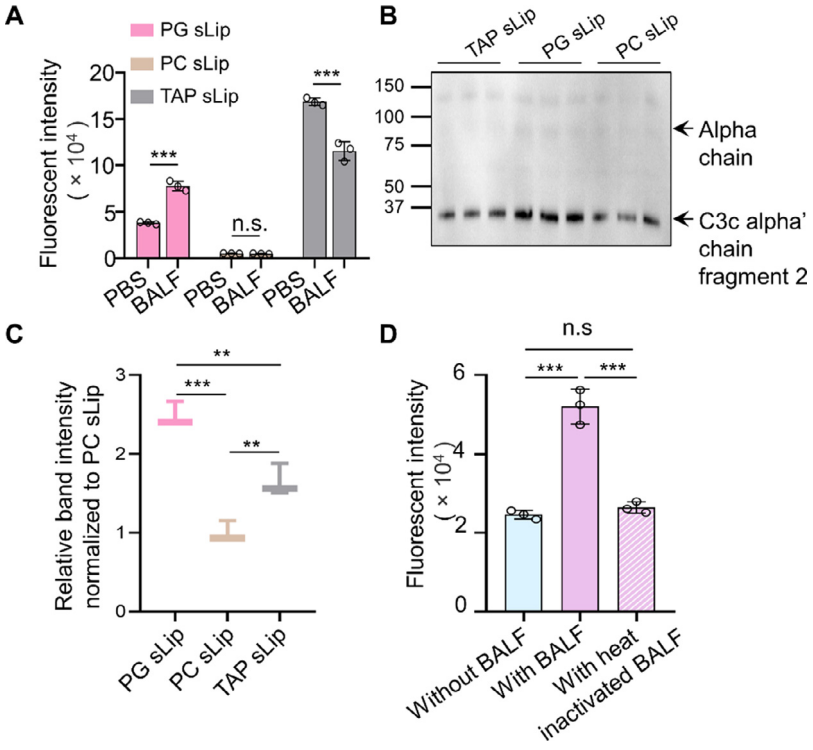

Fig. 6 – Effect of complement in the BALF in mediating interaction between liposomes and MRSA. (A) Fluorescent quantification of MRSA bound with liposomes pretreated with PBS or BALF. (B) Western blot of complement C3 adsorbed on the liposome after incubation with BALF. (C) Quantification of adsorbed complement C3 by normalizing gray values. (D) Fluorescent quantification of MRSA bound with DiD-labeled PG sLip preincubated with PBS or mouse BALF or heat inactivated BALF.

consistent with previous reports that complement protein constitutes an important part of the protein corona opsonized on liposomes [32]. Meanwhile, a remarkable enrichment of complement on PG sLip was observed (Fig. 4E). As known, complement components could also deposit on the bacterial surface when the internal thioester reacts with hydroxyl or amino groups on the cell wall, promoting the phagocytosis and clearance through complement receptors [33]. We therefore sought to examine whether the enhanced bacterial binding is mediated by complement components. Since most of the proteins constituting the complement system are heat-labile, here the serum was heated to 56 °C to inactivate the complement. MRSA bacteria were incubated with fluorescent-labeled PG sLip pretreated with PBS, serum or heat-inactivated serum, respectively. It was confirmed that serum preincubation significantly enhanced liposomal binding to bacteria. However, upon the heat-inactivated serum preincubation, the amount of liposome bound on the surface of bacteria was reduced to the comparable level to that without serum preincubation (Fig. 4F). These results indicated the involvement of complement protein during the interaction process between PG sLip and MRSA bacteria.

It was speculated that almost all liposomes could activate the complement system when exposed to serum under appropriate conditions. SRBC hemolysis assay was conducted to detect the complement activation by all three populations of liposomes. Rat serum was incubated with various liposomes and the residual complement hemolytic activity was assessed. The more complement proteins consume, the more reduction of SRBC hemolytic level induced by the remaining complement occurs. As depicted in Fig. 4G, PG sLip exhibited much stronger complement activation ability than PC sLip and TAP sLip as reported [34]. The activation of complement system could further amplify complement fragments deposition on the surfaces of liposomes, which might provide the explanation of why much complement adsorbed on the PG sLip. All these results suggested that the deposited complement produced by strong cascade activation played a critical role in mediating the interaction between PG sLip and MRSA.

3.5. *PG sLip/Van exhibited superior therapeutic efficacy against MRSA infected osteomyelitis*

Osteomyelitis caused by MRSA infection has been generally considered one of the most difficult-to-treat orthopedic complications in clinical practice. Typical treatment for osteomyelitis includes surgical debridement of infected tissues combined with prolonged antimicrobial therapy to control infection [35]. Due to the biofilm formation at the site of chronic infection, maintenance of high antibiotic concentration in the bone is preferred for effective treatment. Given the robust binding of PG sLip to MRSA planktonic bacteria and biofilm, the therapeutic efficacy of

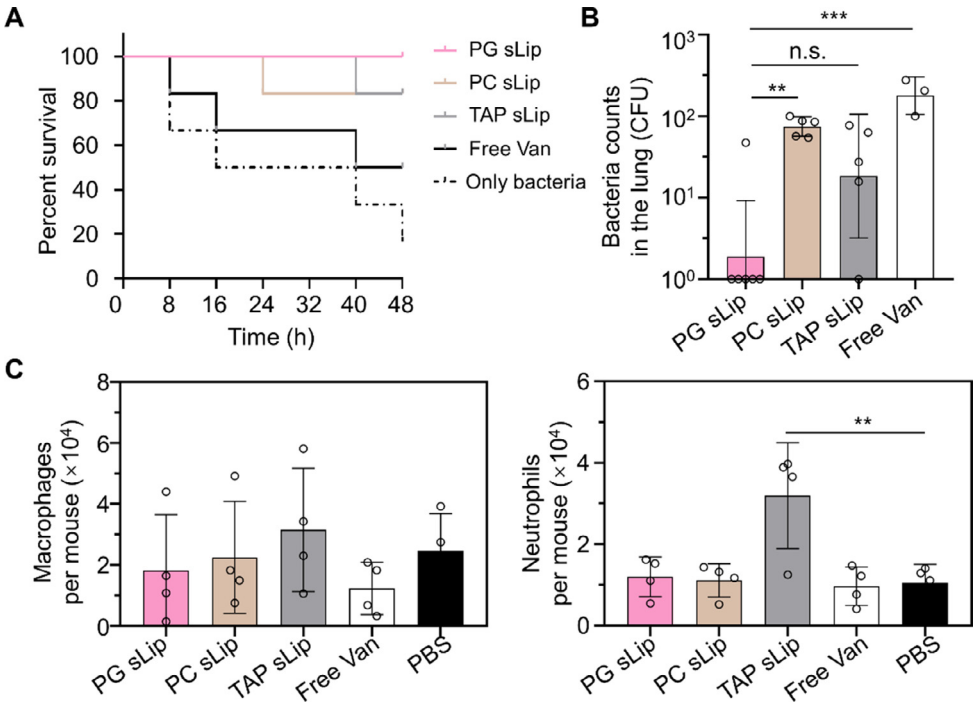

Fig. 7 – *In vivo* therapeutic efficacy in a MRSA pulmonary infected mouse model and safety evaluation. (A) Survival curves of mice with MRSA pneumonia ($n = 6$) that intratracheally administered of liposomal vancomycin. (B) Bacterial load in the lungs at 48 h after treatments ($n = 3–6$). (C) Macrophages and neutrophils count in BALF at 24 h post intratracheal administration ($n = 4$).

PG liposomal vancomycin was evaluated in an *S. aureus*-related osteomyelitis mice model. Firstly, vancomycin-loaded liposomes including PG sLip/Van, PC sLip/Van, and TAP sLip/Van were fabricated and characterized. The sizes of the resulting vancomycin-loaded liposomes were similar to the ones without vancomycin loading (Supplementary Fig. S4). The loading capacity was respective 5.88% for PG sLip, 5.33% for PC sLip, and 5.55% for TAP sLip. The *in vitro* stability of all three populations of liposomes was explored in terms of sizes. The results suggested that they were physically stable over one-week of storage at 4 degree. *In vitro* cumulative release of vancomycin was approximately 20.87% for PG sLip, 22.14% for PC sLip, and 28.03% for TAP sLip after 48 h. No burst release of encapsulated vancomycin occurred for all liposomes. PG sLip/Van, PC sLip/Van, TAP sLip/Van, and free vancomycin were intravenously injected into *S. aureus*-related osteomyelitis mice. The femurs were collected and subjected to bacterial enumeration at 4 h post-treatment. As depicted in Fig. 5A and 5B, free or liposome-formulated vancomycin showed a bactericidal effect toward MRSA infection. PG sLip/Van exhibited superior bactericidal efficacy as demonstrated by significantly reduced number of bacterial colonies in comparison to other groups. Although, it was found from the pharmacokinetic studies that the PG sLip displayed a relative shorter circulation time than PC sLip (Fig. S5), owing to robust binding of PG sLip to MRSA planktonic bacteria and biofilm in the serum-containing condition, it is speculated that PG sLip/Van might be more favorably adhere to MRSA in the infection site, resulting in better antibacterial effects.

In vivo, the potential toxicity of different vancomycin-loaded liposomes was assessed by blood routine examination and hepatic/renal function analysis. A significant decrease of white blood cells and platelet counts in the blood of TAP sLip/Van treated mice was observed, while no obvious difference in blood routine parameters was found between PG sLip/Van treated groups and that of the PBS group, suggestive of PG sLip/Van a safe liposomal vancomycin formulation for the treatment of MRSA infected osteomyelitis (Fig. 5C). Given commonly reported vancomycin associated nephrotoxicity and massive accumulation of liposomal vancomycin in the liver, we further assessed whether it has any effects on the indexes of liver and kidney functions including ALT, AST, CREA, and BUN. It showed that the indexes of vital hepatic and renal functions remained within the normal range after all formulations except TAP sLip/Van treatment (Fig. 5D). These results suggested that PG sLip/Van in the present dosage showed no significant toxicity.

3.6. *PG sLip/Van demonstrates enhanced bacterial binding in BALF and improved therapeutic efficacy against MRSA pneumonia*

Besides systemic infection, bacterial lung infection is common and serious in certain patients especially those with lung diseases or compromised immune systems. MRSA infection is one of the leading causes of hospital-acquired and healthcare-associated pneumonia [36]. Hence, we further explored the effect of pulmonary protein adsorption on the liposome-bacteria interaction. The binding ability of PG sLip to MRSA

after preincubation with mouse BALF or PBS was explored as aforementioned. In consistency with the results in the serum, bacteria treated with BALF preincubated PG sLip exhibited a twofold increase in fluorescence intensity compared to that with PBS (Fig. 6A). Subsequently, western blotting was carried out to assess the amount of complement C3 and its degraded fragments adsorbed on the surface of liposomes. There is a significant enrichment of complement on PG sLip when compared with PC sLip and TAP sLip (Fig. 6B and 6C). Furthermore, the role of complement in mediating liposome binding to bacteria was studied after heating BALF for 30 min to inactivate the complement components. MRSA bacteria were then incubated with fluorescently labeled PG sLip pretreated with PBS, BALF or heat-inactivated BALF, respectively. After preincubation with BALF, the amount of PG sLip bound on the bacteria was significantly increased, while that was reduced to the same level as the PBS group when pretreated with the heat-inactivated BALF (Fig. 6D). Collectively, these data suggest that the complement in the lung adsorbed on the liposome surface could also mediate strong binding of PG sLip to MRSA.

Owing to the ability of PG sLip-BALF protein complex adhering to the bacteria, it was speculated that it would benefit MRSA pneumonia treatment *in vivo*. Here, the therapeutic efficacies of all groups were evaluated in a MRSA pneumonia mice model. In brief, four groups of mice with MRSA pneumonia were intratracheally administered with PG sLip/Van, PC sLip/Van, TAP sLip/Van and free vancomycin (0.75 mg/kg vancomycin), respectively. Treatment of vancomycin or vancomycin-loaded liposomal formulations could prolong the mice survival. Among the liposomal formulations, PG sLip/Van exhibited much better antibacterial efficacy than PC sLip/Van and free drug, demonstrating significantly reduced bacterial burden in the infected lung (Fig. 7A and 7B). However, it was not advantageous over TAP sLip/Van. Due to the low protein concentration and less moisturized environment in the lung, the positively charged surface of TAP sLip might not be fully shielded, resulting in the reserved binding capacity and efficacy. Furthermore, the toxicity of different formulations was evaluated by counting the macrophages and neutrophils in BALF at 24 h post intratracheal administration (Fig. 7C). The number of neutrophils was significantly increased in the cationic TAP sLip/Van treated lung while no obvious macrophage and neutrophil infiltration were observed in the lung after PG sLip/Van treatment. Although these two vancomycin liposomal formulations displayed similar therapeutic efficacy, PG sLip/Van treatment demonstrated superior safety in the treatment of MRSA pneumonia.

4. Conclusion

The present study revealed the critical role of protein corona in mediating liposome-bacteria interactions and demonstrated anionic DSPG sLip as a potential antibiotic delivery nanocarrier for MRSA infection treatment. It provides an intriguing strategy for enhanced bacterial targeting drug delivery based on lipid composition and subsequently formed protein corona.

Conflicts of interest

The authors declare no conflict of interest.

Acknowledgments

This work is supported by the National Natural Science Foundation of China (82125035, 81973245 and 32172894), Shanghai Education Commission Major Project (2021–01–07–00–07-E00081). We would like to thank the National Center for Protein Science Shanghai for the Cryo-EM.

Supplementary materials

Supplementary material associated with this article can be found, in the online version, at doi:10.1016/j.ajps.2022.10.003.

REFERENCES

[1] Jernigan JA, Hatfield KM, Wolford H, Nelson RE, Olubajo B, Reddy SC, et al. Multidrug-resistant bacterial infections in U.S. hospitalized patients, 2012-2017. N Engl J Med 2020;382:1309–19.
[2] Peltola H, Pääkkönen M. Acute osteomyelitis in children. N Engl J Med 2014;370:352–60.
[3] Global burden of bacterial antimicrobial resistance in 2019: a systematic analysis. Lancet 2022;399(10325):629–55.
[4] Ventola CL. The antibiotic resistance crisis: part 1: causes and threats. Pharmacol Ther 2015;40(4):277–83.
[5] Lewis K. The science of antibiotic discovery. Cell 2020;181(1):29–45.
[6] Windels EM, Michiels JE, Fauvart M, Wenseleers T, Van den Bergh B, Michiels J. Bacterial persistence promotes the evolution of antibiotic resistance by increasing survival and mutation rates. ISME J 2019;13(5):1239–51.
[7] Kwon JH, Powderly WG. The post-antibiotic era is here. Science 2021;373(6554):471.
[8] Kavanagh N, Ryan EJ, Widaa A, Sexton G, Fennell J, O'Rourke S, et al. Staphylococcal osteomyelitis: disease progression, treatment challenges, and future directions. Clin Microbiol Rev 2018;31(2) e00084-17.
[9] Baird RW, Douglas NM. Re: epidemiology of escherichia coli bacteraemia: a systematic literature review. Clin Infect Dis 2021;72(9):e435.
[10] Hall-Stoodley L, Costerton JW, Stoodley P. Bacterial biofilms: from the natural environment to infectious diseases. Nat Rev Microbiol 2004;2(2):95–108.
[11] Jamal M, Ahmad W, Andleeb S, Jalil F, Imran M, Nawaz MA, et al. Bacterial biofilm and associated infections. J Chin Med Assoc 2018;81:7–11.
[12] Wu H, Moser C, Wang HZ, Høiby N, Song ZJ. Strategies for combating bacterial biofilm infections. Int J Oral Sci 2015;7(1):1–7.
[13] Nwabuife JC, Pant AM, Govender T. Liposomal delivery systems and their applications against staphylococcus aureus and methicillin-resistant staphylococcus aureus. Adv Drug Deliv Rev 2021;178:113861.
[14] Dos Santos Ramos MA, Dos Santos KC, da Silva PB, de Toledo LG, Marena GD, Rodero CF, et al. Nanotechnological strategies for systemic microbial infections treatment: a review. Int J Pharm 2020;589:119780.

[15] Wang Y. Liposome as a delivery system for the treatment of biofilm-mediated infections. J Appl Microbiol 2021;131(6):2626–39.
[16] Gonzalez Gomez A, Hosseinidoust Z. Liposomes for antibiotic encapsulation and delivery. ACS Infect Dis 2020;6(5):896–908.
[17] Sande L, Sanchez M, Montes J, Wolf AJ, Morgan MA, Omri A, et al. Liposomal encapsulation of vancomycin improves killing of methicillin-resistant staphylococcus aureus in a murine infection model. J Antimicrob Chemother 2012;67(9):2191–4.
[18] Li G, Wang M, Ding T, Wang J, Chen T, Shao Q, et al. cRGD enables rapid phagocytosis of liposomal vancomycin for intracellular bacterial clearance. J Control Release 2022;344:202–13.
[19] Jones MN, Song YH, Kaszuba M, Reboiras MD. The interaction of phospholipid liposomes with bacteria and their use in the delivery of bactericides. J Drug Target 1997;5(1):25–34.
[20] Guo R, Liu Y, Li K, Tian B, Li W, Niu S, et al. Direct interactions between cationic liposomes and bacterial cells ameliorate the systemic treatment of invasive multidrug-resistant staphylococcus aureus infections. Nanomedicine 2021;34:102382.
[21] Radovic-Moreno AF, Lu TK, Puscasu VA, Yoon CJ, Langer R, Farokhzad OC. Surface charge-switching polymeric nanoparticles for bacterial cell wall-targeted delivery of antibiotics. ACS Nano 2012;6(5):4279–87.
[22] Lundqvist M, Stigler J, Elia G, Lynch I, Cedervall T, Dawson KA. Nanoparticle size and surface properties determine the protein corona with possible implications for biological impacts. Proc Natl Acad Sci USA 2008;105(38):14265–70.
[23] Tenzer S, Docter D, Kuharev J, Musyanovych A, Fetz V, Hecht R, et al. Rapid formation of plasma protein corona critically affects nanoparticle pathophysiology. Nat Nanotechnol 2013;8(10):772–81.
[24] Hadjidemetriou M, McAdam S, Garner G, Thackeray C, Knight D, Smith D, et al. The human *in vivo* biomolecule corona onto PEGylated liposomes: a proof-of-concept clinical study. Adv Mater 2019;31(4):e1803335.
[25] Yang M, Wu E, Tang W, Qian J, Zhan C. Interplay between nanomedicine and protein corona. J Mater Chem B 2021;9(34):6713–27.
[26] Ding T, Guan J, Wang M, Long Q, Liu X, Qian J, et al. Natural IgM dominates *in vivo* performance of liposomes. J Control Release 2020;319:371–81.
[27] Mohamed M, Abu Lila AS, Shimizu T, Alaaeldin E, Hussein A, Sarhan HA, et al. PEGylated liposomes: immunological responses. Sci Technol Adv Mater 2019;20(1):710–24.
[28] Schöttler S, Becker G, Winzen S, Steinbach T, Mohr K, Landfester K, et al. Protein adsorption is required for stealth effect of poly(ethylene glycol)- and poly(phosphoester)-coated nanocarriers. Nat Nanotechnol 2016;11(4):372–7.
[29] Caracciolo G, Pozzi D, Candeloro De Sanctis S, Laura Capriotti A, Caruso G, Samperi R, et al. Effect of membrane charge density on the protein corona of cationic liposomes: interplay between cationic charge and surface area. Appl Phys Lett 2011;99:033702.
[30] Stewart PS, Costerton JW. Antibiotic resistance of bacteria in biofilms. Lancet 2001;358(9276):135–8.
[31] Dong D, Thomas N, Thierry B, Vreugde S, Prestidge CA, Wormald PJ. Distribution and inhibition of liposomes on staphylococcus aureus and pseudomonas aeruginosa biofilm. PLoS ONE 2015;10(6):e0131806.
[32] Chu Y, Tang W, Zhang Z, Li C, Qian J, Wei X, et al. Deciphering protein corona by scFv-based affinity chromatography. Nano Lett 2021;21(5):2124–31.
[33] Law SK, Dodds AW. The internal thioester and the covalent binding properties of the complement proteins C3 and C4. Protein Sci 1997;6(2):263–74.
[34] Chonn A, Cullis PR, Devine DV. The role of surface charge in the activation of the classical and alternative pathways of complement by liposomes. J Immunol 1991;146(12):4234–41.
[35] Rao N, Ziran BH, Lipsky BA. Treating osteomyelitis: antibiotics and surgery. Plast Reconstr Surg 2011;127(Suppl 1):177s–87s.
[36] Defres S, Marwick C, Nathwani D. MRSA as a cause of lung infection including airway infection, community-acquired pneumonia and hospital-acquired pneumonia. Eur Respir J 2009;34(6):1470–6.